06ADSC-026

Estimation of Critical Tire Parameters Using GPS Based Sideslip Measurements

David M. Bevly, Robert Daily, and William Travis
Department of Mechanical Engineering, Auburn University

ABSTRACT

This paper investigates the use of GPS to estimate vehicle sideslip and tire information. Both a one antenna GPS antenna/receiver and dual GPS antenna method are studied. Analysis of the accuracy that can be achieved using the two different GPS solutions is provided. The algorithms are then validated on a fully instrumented Infiniti G35 sedan. Experimental data is given showing the performance of the GPS based sideslip estimates compared against a simple bicycle model and a Datron™ velocity sensor.

NOMENCLATURE

r	Vehicle yaw rate
b_{gyro}	Yaw gyro bias
b_a	Longitudinal accelerometer bias
ψ	Orientation of the vehicle centerline (vehicle heading)
ψ_{KF}	Kalman Filter estimate of the vehicle heading
ψ_{GPS}	Two antenna GPS measurement of the vehicle heading
r_{gyro}	Yaw gyro sensor reading
ψ_{GPS}^{Vel}	Horizontal GPS velocity vector heading (vehicle course)
β	Vehicle sideslip angle at the C.G.
β_A	Sideslip angle at the GPS antenna
β_P	Sideslip angle at point P on the vehicle
$\beta_{f,r}$	Sideslip angle at the front and rear axle
V_A	Velocity vector at the GPS antenna
V_P	Velocity vector at point P on the vehicle
$R_{A/P}$	Position vector from the GPS antenna to point P on the vehicle
$V_{x,y}$	Longitudinal and lateral velocity
$\alpha_{x,y}$	Front and rear tire slip angles
$C_{\alpha f,\alpha r}$	Front and rear tire cornering stiffness
a	Distance from the front axle to the vehicle C.G.
b	Distance from the rear axle to the vehicle C.G.
I_z	Vehicle yaw moment of inertia
m	Vehicle mass
δ	Front steer angle

1. INTRODUCTION

Sideslip estimation is a critical aspect of many Electronic Stability Control (ESC) systems [1-3]. Additionally, many ESC systems rely on model parameters of the vehicle and tire to perform optimally. Information on the state of the vehicle such as the location of the center of gravity, cornering stiffnesses, etc. can be estimated using GPS.

Methods using GPS and inertial measurement unit (IMU) integration have been developed to predict critical tire parameters in the limits of handling. Previously GPS/IMU solutions have been shown to estimate vehicle sideslip angle and tire slip angle [4-6]. Using these estimates, the tire cornering stiffness can be estimated for the linear region of the tire. This work expands that research into the nonlinear region of the tire by estimating the lateral force and tire slip angle over the entire operating range. This tire information could be used to improve electronic stability control (ESC) systems.

This paper also shows that although the linear bicycle model describes the vehicle dynamics during some maneuvers, it cannot adequately capture the vehicle behavior during aggressive driver inputs.

To validate this research the algorithms are tested on an Infiniti G35 outfitted with a data acquisition system measuring among other things steer angle, lateral acceleration, roll and yaw rates, and GPS position and velocity. A dual antenna GPS system is also implemented which measures true roll angle and heading. The methods are validated in simulation as well as with experimental data. Experiments are performed on low coefficient of friction surfaces in order to generate excessive sideslip to further validate the

method of using GPS in the non-linear vehicle handling region. The importance of GPS based sideslip measurements and tire parameter estimation is also shown in this paper.

2. VEHICLE MODEL

Figure 1 shows a simple schematic of a vehicle known as the bicycle model. The model neglects weight transfer from inner to outer tires and assumes the same tires and slip angles on the inner and outer wheels [7].

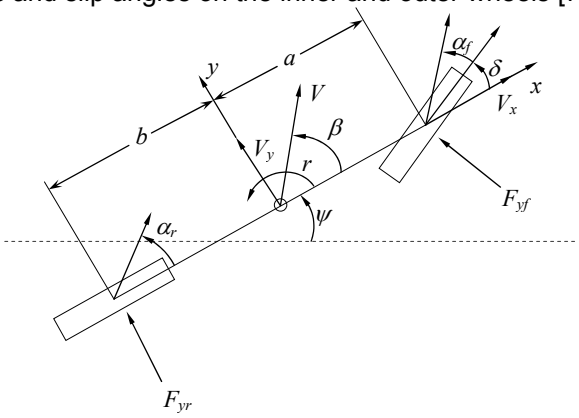

Figure 1. Bicycle model

The state space equations for the lateral dynamics of the bicycle model are given in Equation (1). Note that the effects of weight transfer and road bank are ignored in this state space system of the lateral dynamics. Additionally, the linear dynamics expressed in Equation (1) assume small angles and utilize a linear tire model.

$$\begin{bmatrix}\dot{\beta}\\ \dot{r}\end{bmatrix}=\begin{bmatrix}\frac{-C_{\alpha f}-C_{\alpha r}}{mV} & \frac{-aC_{\alpha f}+bC_{\alpha r}}{mV^2}-1\\ \frac{-aC_{\alpha f}+bC_{\alpha r}}{I_z} & \frac{a^2C_{\alpha f}+b^2C_{\alpha r}}{I_zV}\end{bmatrix}\begin{bmatrix}\beta\\ r\end{bmatrix}+\begin{bmatrix}\frac{C_{\alpha f}}{mV}\\ \frac{aC_{\alpha f}}{I_z}\end{bmatrix}\delta \qquad (1)$$

The body sideslip angle (β in Figure 1) is the difference between the vehicle heading and direction of travel measured at the center of gravity (CG). GPS velocity measurements are used to determine the direction of travel to provide the sideslip measurement:

$$\beta=\psi_{GPS}^{Vel}-\psi \qquad (2)$$

The vehicle heading can be estimated using a yaw gyro. The gyro is initialized and its bias estimated during periods of straight driving, and then integrated during turning maneuvers to provide the vehicle heading. Alternatively, the vehicle heading can be measured using two GPS antennas [8-10]. By utilizing two antennas, heading estimate errors due to both gyro integration (arising from bias estimate errors, scale factor, integration routine and integration of a noisy signal) and synchronization of the GPS/INS measurements are eliminated. The relationship between the lateral velocity (V_y) and the vehicle sideslip is simply:

$$V_y^{GPS}=V^{GPS}\sin(\beta) \qquad (3)$$

The measured slip angle is the slip angle of the vehicle at the antenna. In contrast, it is usually desired to know the slip angle either at the vehicle CG or at the tires. In order to move the slip angle estimation from the GPS antenna to any point (P) on the vehicle, the velocity at the antenna (A) must be transposed to that point with the addition of any velocity arising from vehicle angular velocity as seen in equation (4).

$$\vec{V}_P=\vec{V}_A+\vec{\omega}\times\vec{R}_{A/P} \qquad (4)$$

where $\vec{\omega}$ normally includes roll, pitch, and yaw rates of the vehicle. In this work only the yaw rate was utilized in this correction, with roll and pitch assumed negligible (a planar model). Greater accuracy could be obtained for vehicles with large amounts of roll by subtracting out the component of velocity caused by vehicle roll in the GPS velocity measurements. This would require a roll gyro, however, which is not usually found in stability control systems. The slip angle at point (P) on the vehicle can then be calculated from the velocity components in each axis of the vehicle at that point according to equation (5).

$$\beta_P=\tan^{-1}\left(\frac{V_y^P}{V_x^P}\right) \qquad (5)$$

where V_x and V_y are the velocity components in the body fixed coordinates.

A tire slip angle (α_f and α_r in Figure 1) is the difference between the tire's longitudinal axis and its direction of travel. The direction of travel of each tire can be calculated by translating the vehicle velocity at the GPS antenna to the tire using equation (4). The direction of the rear tire axes is equal to the vehicle heading, while the direction of the front tires is calculated by adding in the steering angle. Ignoring camber effects, the slip angles of the front and rear tires can be found by moving the sideslip angle to the tire and incorporating the measurement of the steer angle:

$$\begin{aligned}\alpha_f&=\beta_f^{tire}-\delta\\ \alpha_r&=\beta_r^{tire}\end{aligned} \qquad (6)$$

3. ESTIMATION OF TIRE PARAMETERS

The lateral accelerations from the accelerometer (minus the accelerometer bias from the Kalman filter estimation algorithm) and the yaw rate measurements can be used with the GPS based tire sideslip angle measurements to provide an estimate of the front and rear tire cornering stiffness. Estimates of the tire cornering stiffness can be obtained various ways, including analyzing the forces of the bicycle model (shown in Figure 1) using Newton's equations and assuming level ground.

$$\begin{aligned}\sum F_y&=m\ddot{y}=F_{yr}+F_{yf}\cos(\delta)\\ \sum M_z&=I_z\ddot{\psi}=-bF_{yr}+aF_{yf}\cos(\delta)\end{aligned} \qquad (7)$$

The two above equations can be solved simultaneously for the lateral front and rear tire forces. The lateral tire forces are then simply a function of the cornering stiffness

$$\begin{aligned} F_{yf} &= 2C_{\alpha f}\alpha_f \\ F_{yr} &= 2C_{\alpha r}\alpha_r \end{aligned} \tag{8}$$

The factor of 2 in the above equation is due to the fact the bicycle model lumps the left and right tires together. Alternatively, the two equations in the bicycle model given in Equation (1) can be used to solve for the estimates of the front and rear cornering stiffnesses. It is important to note that both methods assume the tire is in the linear operating region.

4. SIDESLIP ESTIMATION

The GPS measurement of heading can be combined with inertial measurements through various types of estimators, depending on the measurements available. The purpose of combining the GPS measurements with inertial measurements is to provide high-update rate, unbiased, accurate estimates of the lateral vehicle dynamics.

One of the current ways to combine the GPS heading measurements with the information provided from the yaw gyroscope is through a kinematic or indirect Kalman filter [11,12]. The term kinematic comes from the fact that the model used by the estimator is based solely on the kinematic relationship between the sensors, and not a dynamic model of the vehicle. The state space form for the kinematic relationships is given in Equation (9):

$$\begin{aligned} \dot{X} &= \begin{bmatrix} \dot{\psi} \\ \dot{b}_{gyro} \end{bmatrix} = \begin{bmatrix} 0 & -1 \\ 0 & 0 \end{bmatrix} \begin{bmatrix} \psi \\ b_{gyro} \end{bmatrix} + \begin{bmatrix} 1 \\ 0 \end{bmatrix} r \\ y &= \begin{bmatrix} 1 & 0 \end{bmatrix} \begin{bmatrix} \psi \\ b_{gyro} \end{bmatrix} \text{ or } y = \begin{bmatrix} 0 & 0 \end{bmatrix} \begin{bmatrix} \psi \\ b_{gyro} \end{bmatrix} \end{aligned} \tag{9}$$

Additionally, the measurement noise covariance matrix and the discrete process noise covariance matrix are given in Equation (10):

$$\begin{aligned} R_d &= \begin{bmatrix} \sigma^2_{v_{gps}} & 0 \\ 0 & \sigma^2_{bias} \end{bmatrix} \\ Q_d &= T_s I \begin{bmatrix} T_s\sigma^2_{gyro} & 0 \\ 0 & \sigma^2_{bias} \end{bmatrix} I \end{aligned} \tag{10}$$

The Kalman filter is then applied to the system described by Equation (9). Between GPS measurements and during GPS outages, the Kalman filter simply integrates the yaw rate gyro measurements. When GPS is available, the course measurements are used to estimate the yaw rate gyro bias and zero out the sideslip estimate errors that occur from sensor drift. It is important that only small sideslip angles are encountered when estimating the sensor bias. The sideslip can corrupt the bias estimate and introduce errors, which can propagate to other states [13].

The Kalman Filter (KF) is comprised of a measurement update and time update [14], which is performed at each time step (k). The measurement update is described by:

$$\begin{aligned} L_k &= P_k C^T (CP_k C^T + R)^{-1} \\ X_k &= X_k + L_k (y_k - CX_{k-n}) \\ P_k &= (I - L_k C) P_k \end{aligned} \tag{11}$$

where: L = Kalman Gain Vector
P = State Estimation Covariance Matrix
C = Observation Matrix
R = Sensor Noise Vector
I = Identity Matrix
X = State Estimate Vector
k = current time index
n = age of the GPS measurement (in samples)

A simple trapezoidal integration time update is described by:

$$\begin{aligned} X_{k+1} &= X_k + \frac{\Delta t}{2}\left(\dot{X}_{k+1} + \dot{X}_k\right) \\ P_{k+1} &= \Phi P_k \Phi^T + Q_w \end{aligned} \tag{12}$$

where: $\dot{X}_k$ is calculated from the linear equation in (9)
Φ_k is the discretized Jacobian at each time step
Q_w is the discretized process noise matrix

The trapezoidal (or higher order) integration technique is essential to reduce the amount of error in the vehicle heading estimate. When no current GPS measurements are available the filter uses the time update step (Equation 12) to integrate forward and estimate the vehicle heading from the gyro yaw rate measurement. The Kalman filter provides a current estimate of the vehicle sideslip, as opposed to the latent GPS measurement by itself. As noted earlier, it is important that the GPS measurements be compared with heading estimates of the same age in the measurement update.

In the kinematic Kalman filter, the two states being estimated are the heading of the vehicle and the bias on the yaw rate gyroscope which is modeled as a random walk. The yaw rate acquired from the gyroscope is used as an input into the system. During straight driving, the observation matrix (C) is set to $\begin{bmatrix} 1 & 0 \end{bmatrix}$ in order to estimate the bias on the gyroscope by using the GPS course measurement. GPS course is the heading of the vehicle plus sideslip which is assumed to be zero during straight driving. The observation matrix is then set to $\begin{bmatrix} 0 & 0 \end{bmatrix}$ during turning or during periods when GPS is lost. Setting the observation matrix to zero during turning effectively turns off the gyro bias estimation and integrates the yaw gyroscope (with the bias removed) in

order to provide an estimate of the true vehicle heading. It is important to note that this can lead to estimation errors in the presence of gyroscope scale factor errors or during periods of long integration. Although the kinematic Kalman filter does not provide a direct estimate of vehicle sideslip, an estimate of sideslip can be obtained by comparing the difference between GPS course angle and the estimated heading of the vehicle from integrating the bias free gyro. The equation for this sideslip estimate can be seen below in Equation (13).

$$\hat{\beta} = \nu_{GPS} - \hat{\psi}_{Kf} \tag{13}$$

Alternatively, a dual antenna can be used to provide estimates of vehicle heading. The GPS measurements from a dual antenna system can be combined with the inertial sensors using a kinematic estimator.

$$\begin{bmatrix} \dot{\psi} \\ \dot{\beta} \\ \dot{b}_{gyro} \end{bmatrix} = \begin{bmatrix} 0 & 0 & -1 \\ 0 & 0 & 0 \\ 0 & 0 & 0 \end{bmatrix} \begin{bmatrix} \psi \\ \beta \\ b_{gyro} \end{bmatrix} + \begin{bmatrix} 1 \\ 0 \\ 0 \end{bmatrix} r$$

$$y = \begin{bmatrix} 1 & 0 & 0 \\ 1 & 1 & 0 \end{bmatrix} \begin{bmatrix} \psi \\ \beta \\ b_{gyro} \end{bmatrix} \tag{14}$$

Additionally, a lateral accelerometer can be integrated into the estimator. However the accelerometer measurement must be corrected for roll and centripetal acceleration.

$$\begin{bmatrix} \dot{\psi} \\ \dot{\beta} \\ \dot{b}_{gyro} \\ \dot{b}_a \end{bmatrix} = \begin{bmatrix} 0 & 0 & -1 & 0 \\ 0 & 0 & 0 & -V_x \\ 0 & 0 & 0 & 0 \\ 0 & 0 & 0 & 0 \end{bmatrix} \begin{bmatrix} \psi \\ \beta \\ b_{gyro} \\ b_a \end{bmatrix} + \begin{bmatrix} 1 & 0 \\ 0 & V_x \\ 0 & 0 \\ 0 & 0 \end{bmatrix} \begin{bmatrix} r & a_y \end{bmatrix}$$

$$y = \begin{bmatrix} 1 & 0 & 0 & 0 \\ 1 & 1 & 0 & 0 \end{bmatrix} \begin{bmatrix} \psi \\ \beta \\ b_{gyro} \\ b_a \end{bmatrix} \tag{15}$$

$$a_y = a_y^{accel} - g\sin(\theta) - V(r - b_{gyro})$$

The same Kalman filter equations given in (11-12) are used to update the estimates in both of the systems described in Equation (14) and Equation (15).

Alternative methods that utilize a vehicle model can be used to estimate the sideslip [15-17]. However, the accuracy of these methods is dependent upon the resolution of the model and accurate knowledge of the vehicle parameters.

THEORETICAL PERFORMANCE

The sideslip accuracy is a function of the lateral velocity accuracy and the overall vehicle speed as shown below.

$$\sigma_\beta = \frac{\sigma_{V_y}}{V} \tag{16}$$

Similarly, the GPS velocity-based course measurement depends on the GPS velocity accuracy (~ 5 cm/s) and the vehicle speed.

$$\sigma_\nu = \frac{\sigma_V}{V} \tag{17}$$

Since the sideslip is simply the difference in the yaw and course measurements, the sideslip accuracy can also be related to the accuracy of the course and yaw measurements.

$$\sigma_\beta = \sqrt{\sigma_\nu^2 + \sigma_\psi^2} \tag{18}$$

The Kalman filter used to blend the GPS and INS measurements provides an estimate of the accuracy of each state in the state estimation covariance matrix (P). The estimated one-sigma accuracy of the lateral velocity (V_y) estimate can be determined by taking the expectation of GPS velocity standard deviation multiplied with the term associated with the sideslip state in the covariance matrix (P) as it is updated in the Kalman filter. The resulting sideslip angle accuracy can be determined using Equations (16-18). Figure 2 shows the covariance analysis results for the GPS/INS estimated sideslip accuracy. At time = 50 seconds, the second GPS antenna is turned off to provide the estimated slip angle accuracy using only one GPS antenna. The growth in the slip angle for t > 50 seconds is due to the error growth from the integrated gyro heading which is then added to the GPS course error as shown in Equation (18). The covariance analysis shows that even the one antenna GPS/INS can provide sideslip angles with accuracies of 0.37 degrees for maneuvers up to 50 seconds. The band in the covariance plot is due to the accelerometer drift between 5 Hz GPS measurements. The covariance analysis is further validated with experimental data in the next section.

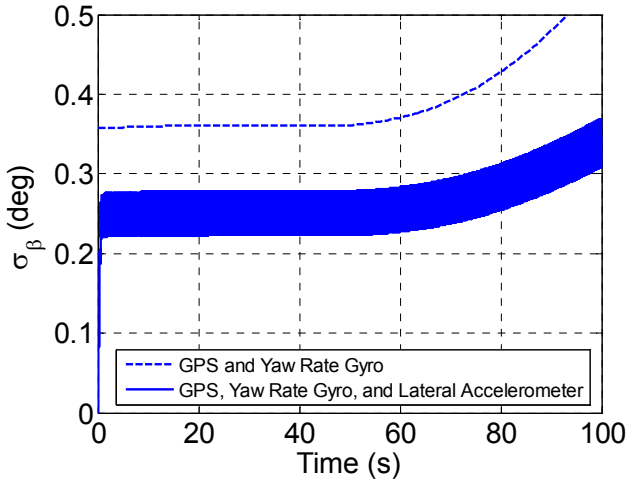

Figure 2. Covariance estimate of sideslip angle measurement at 8 m/s.

The covariance values shown in Figure 2 up to t = 50 seconds represent the errors using the 2 antenna method. The error growth after t = 50 seconds represents the covariance analysis from one GPS antenna (and integrating a yaw gyro). A summary of the covariance analysis (given in terms of the 1-σ values) is shown in Table I. It is important to note that these covariance values assume there are no unmodelled sensor dynamics in the system. Also note that the accuracy of these estimates will improve with speed as seen in Equations (16-18) [5]. To improve the overall accuracy of the estimates, more comprehensive kinematic relationships could be added to reduce errors induced by roll and pitch. Additionally, the analysis shown in Figure 2 and values given in Table I are dependent primarily on the INS sensors, such as sensor noise and bias stability, and not the vehicle model.

Table I. Covariance Analysis Summary (Max 1-σ Values) at 8 m/s

	2-antenna	1-antenna (for a 50 second maneuver)
Vehicle Yaw (no yaw gyro)	0.4 deg	NA
Vehicle Yaw (with yaw gyro)	0.1 deg	< 0.42 deg
GPS Course	0.36 deg	0.36 deg
GPS Slip Angle (no gyro)	0.54 deg	NA
GPS Slip Angle (with yaw gyro)	0.37 deg	< 0.55 deg
GPS + a_y Slip Angle	0.28 deg	< 0.37 deg

EXPERIMENTAL RESULTS

The methods described in the previous section were experimentally tested on a fully instrumented G35 sedan shown in Figure 3. The G35 is equipped with a dual antenna Novatel™ Beeline receiver which provides 5 Hz updates of vehicle heading, roll, and course. The G35 is also instrumented with a Crossbow™ IMU which was recorded at 30 Hz. Additionally, wheel speed and steer angle were recorded from the onboard sensors through the CAN bus.

Figure 3. Instrumented Infiniti G35 sedan

A series of experiments were first performed to validate the GPS based sideslip estimate. A Datron velocity sensor was used to measure the actual sideslip of the vehicle. Figure 4 compares the GPS based sideslip estimate to the Datron measured sideslip during hard cornering maneuvers. Figure 5 further compares the GPS based sideslip estimate to the Datron measured sideslip while driving around a 1.7 mile oval test track at Auburn University. Sideslip was estimated using a single GPS antenna and yaw rate gyro for these experiments.

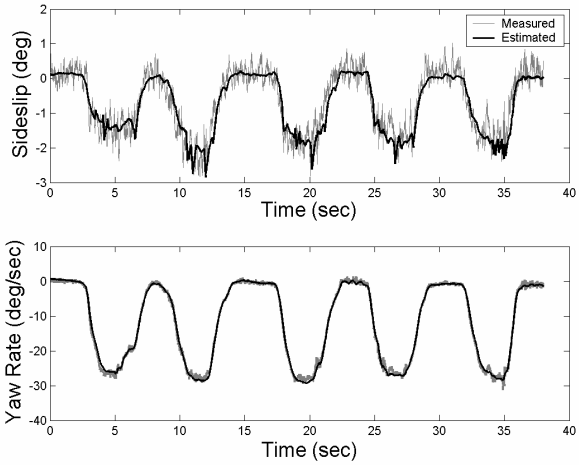

Figure 4. Comparison of measured and estimated sideslip and yaw rate during 8 m/s hard cornering maneuvers.

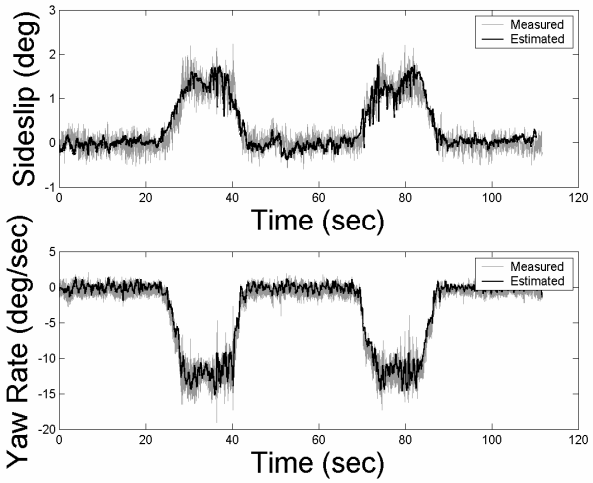

Figure 5. Comparison of measured and estimated sideslip and yaw rate during a 32 m/s lap around the test track.

Figure 6 compares the GPS based sideslip measurement against the bicycle model simulation during a series of lane change maneuvers. Note that the sideslip and yaw rate measurements agree very well with the output predicted by the bicycle model. Figure 7 again compares the GPS based sideslip measurement against the bicycle model simulation during an aggressive slalom maneuver on dry asphalt. Note that in this experiment the measured sideslip from the dual antenna GPS system deviates from the sideslip predicted by the bicycle model during the most extreme part of the experiment. This is due to the fact that the car is no longer operating in the linear range of the tire curve. However, the measured yaw rate continues to match the yaw rate predicted by the bicycle model. Therefore simply observing the vehicle yaw rate may not be adequate to determine the state of the vehicle during some maneuvers. This motivates the need for an actual measurement of sideslip.

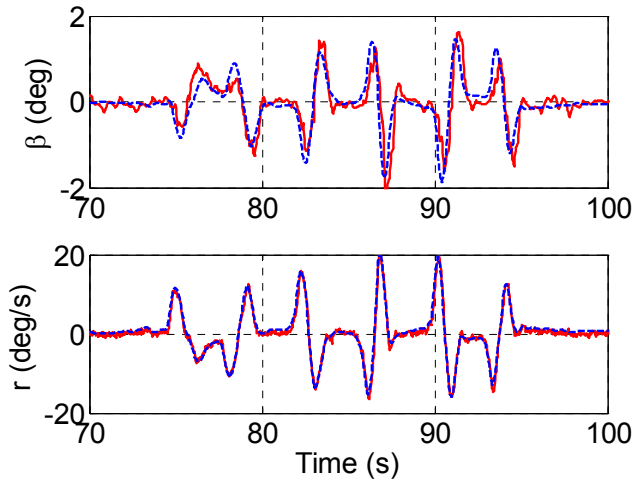

Figure 6. Sideslip and yaw rate during lane change maneuvers at 20 m/s (solid red – measured; dashed blue – bicycle model)

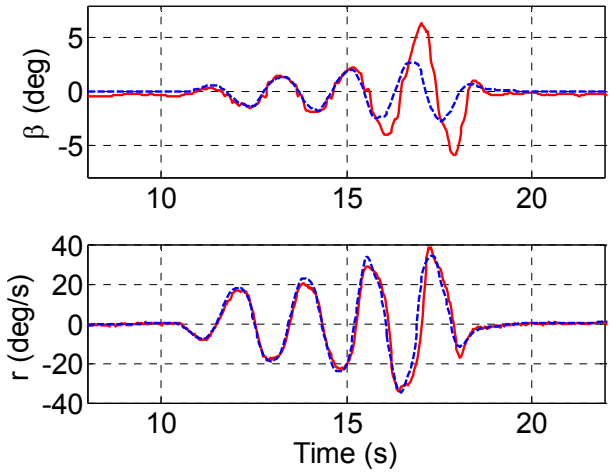

Figure 7. Sideslip and yaw rate during aggressive handling maneuvers at 23 m/s (sold red – measured; dashed blue – bicycle model)

Tire slip angle is found by moving slip angle at the center of gravity to the front and rear axle and accounting for the steer angle. This is done with Equations (4-6). Equation (7) is used to estimate the lateral force at each axle. The tire curve at each axle is then generated using each lateral force with its corresponding slip angle. From the tire curve, the peak lateral force can be seen. The tire cornering stiffness per axle can be determined using the relationship in Equation (8).

Figure 8 shows experimental tire curves obtained using GPS sideslip measurements with the dual antenna system while aggressively driving on dry asphalt. Figures 9 and 10 display the front and rear tire curves, respectively, when the same test was performed on wet asphalt. Control of the car was lost and the rear slid out. The peak lateral force obtained in the rear is lower, and the tire enters the nonlinear region as tire slip increases beyond 4 degrees. Since the G35 is rear wheel drive, the longitudinal slip generated in the rear lowered the total amount of available force. Typically, passenger car tires peak at 8 to 10 degrees of tire slip. The coupling of the longitudinal and lateral slip reduced the slip peak to 4 degrees. It is important to note that these three plots use raw, unfiltered data. The majority of outlying points are due to sensor noise and weight transfer. It is also important to note the tire curves are per axle, not per tire.

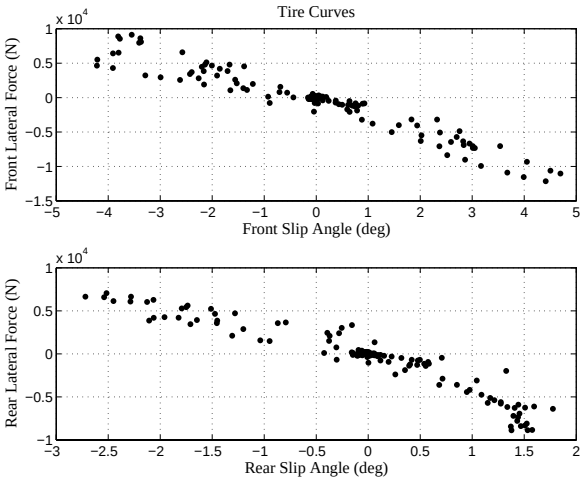

Figure 8. Estimated tire curve data using the GPS measured sideslip on dry asphalt

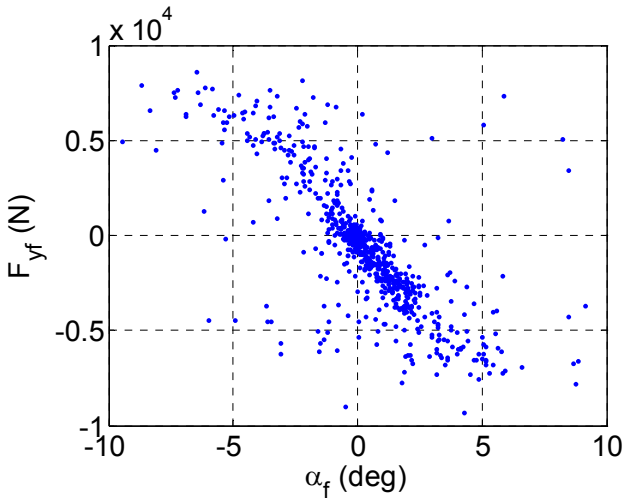

Figure 9. Estimated front tire curve data using the GPS measured sideslip on wet asphalt

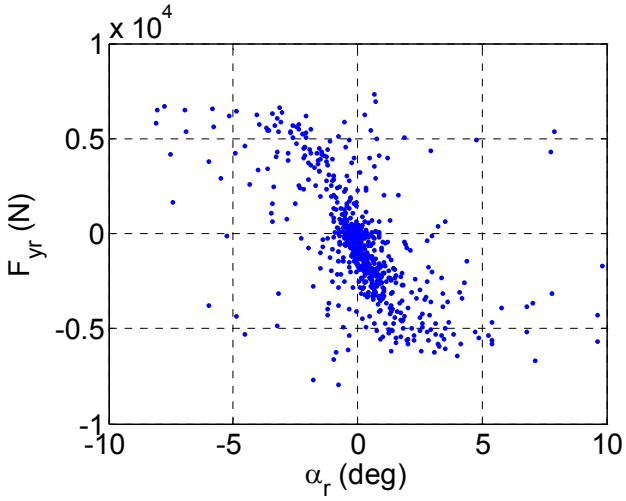

Figure 10. Estimated rear tire curve data using the GPS measured sideslip on wet asphalt

Figure 11 compares the bicycle model with actual measured data of a slalom on wet asphalt at 25 m/s. Sideslip was measured with the dual antenna GPS system. The model breaks down because the peak tire force is exceeded on the wet surface, such that the tires can no longer be approximated without saturation, which causes the vehicle to slide. Figure 12 shows the same data run, but a Dugoff tire model [18] has been inserted into the bicycle model to describe the tire curve more accurately. The peak force and tire cornering stiffness were taken from the non-linear tire curves shown in Figures 9 and 10 and input into the Dugoff tire model. The simulation captures the initial slide of the vehicle (as seen in the sideslip and yaw rate plots), until the small angle assumptions are invalid.

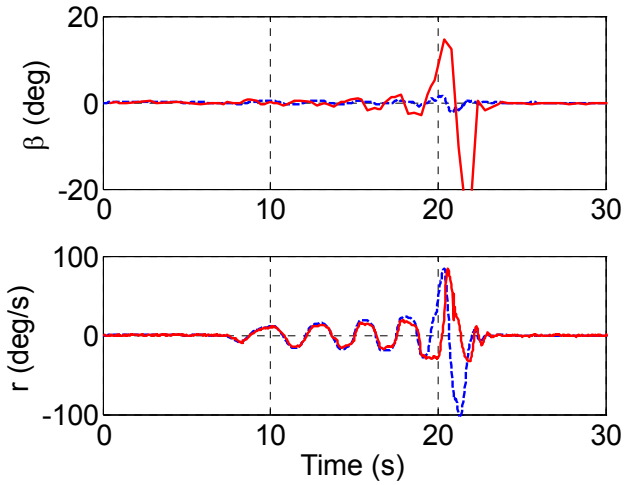

Figure 11: Sideslip and yaw rate during slalom handling maneuvers at 25 m/s on wet asphalt (sold red – measured; dashed blue – bicycle model with linear tire model)

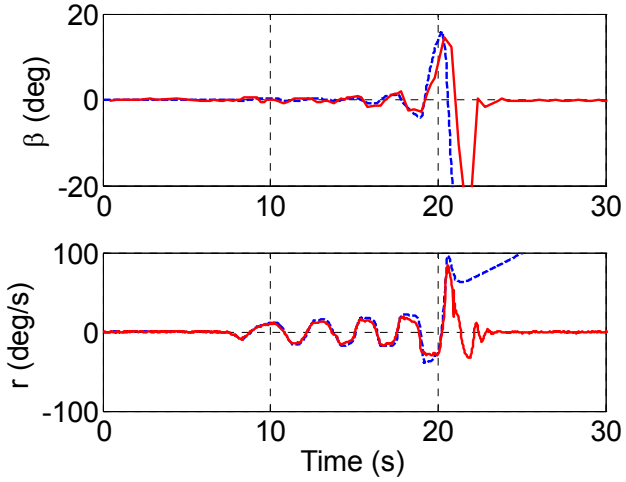

Figure 12: Sideslip and yaw rate during slalom handling maneuvers at 25 m/s on wet asphalt (sold red – measured; dashed blue – bicycle model with non-linear Dugoff tire model)

CONCLUSION

This paper has shown the ability of GPS to provide accurate measurements of vehicle sideslip for use in Electronic Stability Control Systems. A method for integrating inertial sensors with one or two antenna GPS systems was provided. Analysis of the sideslip accuracy

was provided. The algorithms were then validated using an experimental vehicle test bed. The experiments showed the effectiveness of the GPS measurements to provide critical vehicle information for ESC systems.

ACKNOWLEDGMENTS

The authors would like to thank Nissan North America for the loan of the Infiniti G35 sedan for the vehicle tests. Additionally, the authors would like to thank Delphi for the loan of the Datron velocity sensor used for validating some of the GPS/INS sideslip measurements. Any opinions, findings, conclusions, or recommendations in expressed in this publication are those of the authors and do not necessarily reflect the views of Nissan or Delphi.

REFERENCES

[1] Nishio H., et. al. "Development of Vehicle Stability Control Based on Vehicle Sideslip Angle Estimations," SAE paper No. 2001-01-0137.

[2] Tseng, H. E., et. al. "Technical Challenges in the Development of Vehicle Stability Control System," *Proceeding from the 1999 IEEE International Control Conference on Control Applications*, Kohala Coast-Island of Hawaii, HI, August 1999.

[3] Ray, L. "Nonlinear State and Tire Force Estimation for Advanced Vehicle Control," *IEEE transaction on Control System Technology*, 1995, Vol. 3, No. 1, pp. 117-124.

[4] Bevly, D. M., Gerdes, J. C., Wilson, C. "The Use of GPS Based Velocity Measurements for Measurement of Sideslip and Wheel Slip," *Vehicle System Dynamics*, Vol. 38, No. 2, 2002, pp. 127-147.

[5] Daily, R. Bevly, D. M. "The use of GPS for Vehicle Stability Control Systems," *IEEE Transactions of Industrial Electronics*, Vol. 51, No. 2, April 2004.

[6] Bevly, D. M. et. al. "The Use of GPS Based Velocity Measurements for Improved Vehicle State Estimation," *Proceeding from the ACC 2000*, June 2000, Chicago, IL.

[7] Gillespie, T. D.: Fundamentals of Vehicle Dynamics, Society of Automotive Engineers, INC. Warrendale, Pa, 1992.

[8] Ryu, J., Rossetter, E.J., Gerdes, J.C., "Vehicle Sideslip and Roll parameter Estimation Using GPS," *Proceeding of the AVAC 2002*.

[9] Bevly D.M., Sheridan, R., Gerdes, J.C.. "Integrating INS sensors with GPS with GPS Velocity measurements for Continuous Estimation of Vehicle sideslip and Tire Cornering Stiffness," *Proceedings from 2001 ACC.*

[10] Hong, S. et. al. "Estimation of Errors in INS with Multiple GPS Antenna," *Proceeding from the 2001 IEEE Conference on Industrial Electronic Conference*

[11] Bevly, D. M., "GPS: A Low Cost Velocity Sensor for Correcting Inertial Sensor Errors on Ground Vehicles," *Journal of Dynamic Systems, Measurement, and Control*. Vol. 126, No. 2, June 2004.

[12] Ibrahim, F. et. al. "Accurate Gap Filling using Properly Initialized INS During Periods of GPS Signal Blockage," *Proceeding from the 1999 ION-GPS Meetings,* Nashville, TN, September 1999.

[13] Travis, W., Bevly, D.M., "Navigation Errors Introduced by Ground Vehicle Dynamics," *Proceedings of the 2005 ION-GNSS*, Long Beach, CA, September 2005.

[14] Stengel R.: Optimal Control and Estimation, Dover Publications, New York, 1994.

[15] Anderson, R. *Using GPS For Model Based Estimation of Critical Vehicle States and Parameters,* M.S. Thesis, Department of Mechanical Engineering, Auburn University, December 2004.

[16] Farrlly, J., Wellstead P., "Estimation of vehicle Lateral Velocity," *Proceedings from the 1996 IEEE Conference on Control Application*

[17] Rock, K. L., Beiker, S. A., Laws, S., Gerdes, J. C., "Validating GPS Based Measurements for Vehicle Control," *Proceedings of IMECE 2005*, November, 2005, Orlando, FL.

[18] Dugoff, H., Francher, P., and Segel, L., "An Analysis of Tire Traction Properties and Their Influence on Vehicle Dynamic Performance," 1970, SAE Document No. 700377.

CONTACT

David M. Bevly directs the GPS and Vehicle Dynamics Laboratory at Auburn University. His research interests include GPS/INS integration as well as navigation, control and state estimation of vehicle controls Information on the lab's research can be found at http://www.eng.auburn.edu/~dmbevly/gavlab/